

University of Nebraska - Lincoln

DigitalCommons@University of Nebraska - Lincoln

Kenneth Bloom Publications

Research Papers in Physics and Astronomy

2-1-1999

Measurement of the mass splittings between the $b\bar{b}\chi_{b,J}(1P)$ states

K.W. Edwards
Carleton University

Kenneth A. Bloom
University of Nebraska-Lincoln, kbloom2@unl.edu

CLEO Collaboration

Follow this and additional works at: <https://digitalcommons.unl.edu/physicsbloom>

 Part of the [Physics Commons](#)

Edwards, K.W.; Bloom, Kenneth A.; and Collaboration, CLEO, "Measurement of the mass splittings between the $b\bar{b}\chi_{b,J}(1P)$ states" (1999). *Kenneth Bloom Publications*. 141.

<https://digitalcommons.unl.edu/physicsbloom/141>

This Article is brought to you for free and open access by the Research Papers in Physics and Astronomy at DigitalCommons@University of Nebraska - Lincoln. It has been accepted for inclusion in Kenneth Bloom Publications by an authorized administrator of DigitalCommons@University of Nebraska - Lincoln.

Measurement of the mass splittings between the $b\bar{b}\chi_{b,J}(1P)$ states

K. W. Edwards,¹ A. Bellerive,² R. Janicek,² D. B. MacFarlane,² P. M. Patel,² A. J. Sadoff,³ R. Ammar,⁴ P. Baringer,⁴ A. Bean,⁴ D. Besson,⁴ D. Coppage,⁴ C. Darling,⁴ R. Davis,⁴ S. Kotov,⁴ I. Kravchenko,⁴ N. Kwak,⁴ L. Zhou,⁴ S. Anderson,⁵ Y. Kubota,⁵ S. J. Lee,⁵ J. J. O'Neill,⁵ R. Poling,⁵ T. Riehle,⁵ A. Smith,⁵ M. S. Alam,⁶ S. B. Athar,⁶ Z. Ling,⁶ A. H. Mahmood,⁶ S. Timm,⁶ F. Wappler,⁶ A. Anastassov,⁷ J. E. Duboscq,⁷ D. Fujino,^{7,*} K. K. Gan,⁷ T. Hart,⁷ K. Honscheid,⁷ H. Kagan,⁷ R. Kass,⁷ J. Lee,⁷ H. Schwarthoff,⁷ M. B. Spencer,⁷ M. Sung,⁷ A. Undrus,^{7,†} A. Wolf,⁷ M. M. Zoeller,⁷ S. J. Richichi,⁸ H. Severini,⁸ P. Skubic,⁸ M. Bishai,⁹ J. Fast,⁹ J. W. Hinson,⁹ N. Menon,⁹ D. H. Miller,⁹ E. I. Shibata,⁹ I. P. J. Shipsey,⁹ M. Yurko,⁹ S. Glenn,¹⁰ Y. Kwon,^{10,‡} A. L. Lyon,¹⁰ S. Roberts,¹⁰ E. H. Thorndike,¹⁰ C. P. Jessop,¹¹ K. Lingel,¹¹ H. Marsiske,¹¹ M. L. Perl,¹¹ V. Savinov,¹¹ D. Ugolini,¹¹ X. Zhou,¹¹ T. E. Coan,¹² V. Fadeyev,¹² I. Korolkov,¹² Y. Maravin,¹² I. Narsky,¹² V. Shelkov,¹² J. Staeck,¹² R. Stroynowski,¹² I. Volobouev,¹² J. Ye,¹² M. Artuso,¹³ F. Azfar,¹³ A. Efimov,¹³ M. Goldberg,¹³ D. He,¹³ S. Kopp,¹³ G. C. Moneti,¹³ R. Mountain,¹³ S. Schuh,¹³ T. Skwarnicki,¹³ S. Stone,¹³ G. Viehhauser,¹³ J. C. Wang,¹³ X. Xing,¹³ J. Bartelt,¹⁴ S. E. Csorna,¹⁴ V. Jain,^{14,§} K. W. McLean,¹⁴ S. Marka,¹⁴ R. Godang,¹⁵ K. Kinoshita,¹⁵ I. C. Lai,¹⁵ P. Pomianowski,¹⁵ S. Schrenk,¹⁵ G. Bonvicini,¹⁶ D. Cinabro,¹⁶ R. Greene,¹⁶ L. P. Perera,¹⁶ G. J. Zhou,¹⁶ M. Chadha,¹⁷ S. Chan,¹⁷ G. Eigen,¹⁷ J. S. Miller,¹⁷ M. Schmidtler,¹⁷ J. Urheim,¹⁷ A. J. Weinstein,¹⁷ F. Würthwein,¹⁷ D. W. Bliss,¹⁸ D. E. Jaffe,¹⁸ G. Masek,¹⁸ H. P. Paar,¹⁸ S. Prell,¹⁸ V. Sharma,¹⁸ D. M. Asner,¹⁹ J. Gronberg,¹⁹ T. S. Hill,¹⁹ D. J. Lange,¹⁹ R. J. Morrison,¹⁹ H. N. Nelson,¹⁹ T. K. Nelson,¹⁹ D. Roberts,¹⁹ B. H. Behrens,²⁰ W. T. Ford,²⁰ A. Gritsan,²⁰ J. Roy,²⁰ J. G. Smith,²⁰ J. P. Alexander,²¹ R. Baker,²¹ C. Bebek,²¹ B. E. Berger,²¹ K. Berkelman,²¹ K. Bloom,²¹ V. Boisvert,²¹ D. G. Cassel,²¹ D. S. Crowcroft,²¹ M. Dickson,²¹ S. von Dombrowski,²¹ P. S. Drell,²¹ K. M. Ecklund,²¹ R. Ehrlich,²¹ A. D. Foland,²¹ P. Gaidarev,²¹ R. S. Galik,²¹ L. Gibbons,²¹ B. Gittelman,²¹ S. W. Gray,²¹ D. L. Hartill,²¹ B. K. Heltsley,²¹ P. I. Hopman,²¹ J. Kandaswamy,²¹ D. L. Kreinick,²¹ T. Lee,²¹ Y. Liu,²¹ N. B. Mistry,²¹ C. R. Ng,²¹ E. Nordberg,²¹ M. Ogg,^{21,||} J. R. Patterson,²¹ D. Peterson,²¹ D. Riley,²¹ A. Soffer,²¹ B. Valant-Spaight,²¹ C. Ward,²¹ M. Athanas,²² P. Avery,²² C. D. Jones,²² M. Lohner,²² S. Patton,²² C. Prescott,²² J. Yelton,²² J. Zheng,²² G. Brandenburg,²³ R. A. Briere,²³ A. Ershov,²³ Y. S. Gao,²³ D. Y.-J. Kim,²³ R. Wilson,²³ H. Yamamoto,²³ T. E. Browder,²⁴ Y. Li,²⁴ J. L. Rodriguez,²⁴ T. Bergfeld,²⁵ B. I. Eisenstein,²⁵ J. Ernst,²⁵ G. E. Gladding,²⁵ G. D. Gollin,²⁵ R. M. Hans,²⁵ E. Johnson,²⁵ I. Karliner,²⁵ M. A. Marsh,²⁵ M. Palmer,²⁵ M. Selen,²⁵ and J. J. Thaler²⁵

(CLEO Collaboration)

¹Carleton University, Ottawa, Ontario, Canada K1S 5B6
and the Institute of Particle Physics, Canada²McGill University, Montréal, Québec, Canada H3A 2T8
and the Institute of Particle Physics, Canada³Ithaca College, Ithaca, New York 14850⁴University of Kansas, Lawrence, Kansas 66045⁵University of Minnesota, Minneapolis, Minnesota 55455⁶State University of New York at Albany, Albany, New York 12222⁷Ohio State University, Columbus, Ohio 43210⁸University of Oklahoma, Norman, Oklahoma 73019⁹Purdue University, West Lafayette, Indiana 47907¹⁰University of Rochester, Rochester, New York 14627¹¹Stanford Linear Accelerator Center, Stanford University, Stanford, California 94309¹²Southern Methodist University, Dallas, Texas 75275¹³Syracuse University, Syracuse, New York 13244¹⁴Vanderbilt University, Nashville, Tennessee 37235¹⁵Virginia Polytechnic Institute and State University, Blacksburg, Virginia 24061¹⁶Wayne State University, Detroit, Michigan 48202¹⁷California Institute of Technology, Pasadena, California 91125¹⁸University of California, San Diego, La Jolla, California 92093¹⁹University of California, Santa Barbara, California 93106²⁰University of Colorado, Boulder, Colorado 80309-0390²¹Cornell University, Ithaca, New York 14853²²University of Florida, Gainesville, Florida 32611²³Harvard University, Cambridge, Massachusetts 02138²⁴University of Hawaii at Manoa, Honolulu, Hawaii 96822²⁵University of Illinois, Urbana-Champaign, Illinois 61801

(Received 12 March 1998; published 12 January 1999)

We present new measurements of photon energies and branching fractions for the radiative transitions $Y(2S) \rightarrow \gamma \chi_{b(J=0,1,2)}(1P)$. The masses of the χ_b states are determined from the measured radiative photon energies. The ratio of mass splittings between the χ_b substates, $r \equiv (M_{J=2} - M_{J=1}) / (M_{J=1} - M_{J=0})$, with M the χ_b mass, provides information on the nature of the $b\bar{b}$ confining potential. We find $r(1P) = 0.542 \pm 0.022 \pm 0.024$. This value is somewhat lower than the previous world average, but more consistent with the theoretical expectation that $r(1P) < r(2P)$; i.e., that this mass splitting ratio is smaller for the $\chi_b(1P)$ states than for the $\chi_b(2P)$ states. [S0556-2821(99)02903-3]

PACS number(s): 13.40.Hq, 12.39.Jh, 12.39.Pn, 14.40.Gx

The Y particles (bound systems of heavy bottom-quark–bottom-antiquark pairs) play an important role in studies of strong interactions. The bottom-quark–bottom-antiquark pair is a positroniumlike system bound by strong interactions. Because the Y system is nearly non-relativistic ($\beta^2 \approx 0.08$), theory can start from a relatively simple non-relativistic potential model and add relativistic terms as next-order corrections to describe the Y mass-spectrum, as well as the partial widths for the transitions expected within the bottomonium system. Relativistic effects as a result of spin-orbit and tensor interactions generate fine splittings; hyperfine splittings arise from spin-spin interactions. Potential models predict electric dipole transitions $Y(2S) \rightarrow \gamma \chi_{b,J}(1P)$ with rates proportional to $(2J+1)E_\gamma^3$, with E_γ the photon energy. These transitions have already been investigated in four experiments—CUSB [1], CLEO [2], Crystal Ball [3] and ARGUS [4]—by measuring the energy distribution of transition photons detected inclusively in multi-hadronic events: $Y(2S) \rightarrow \gamma \chi_{b,J}(1P)$, $\chi_{b,J}(1P) \rightarrow$ hadrons. The exclusive radiative cascade transitions, $Y(2S) \rightarrow \gamma \chi_{b,J}(1P)$, $\chi_{b,J}(1P) \rightarrow \gamma Y(1S)$, in which the $Y(1S)$ is tagged by its decay to dileptons, were measured by the CUSB [5] and Crystal Ball [6] experiments.

In the present analysis, we have used the inclusive method to study the radiative photon transitions between the $Y(2S)$ and the $\chi_{b,J}(1P)$ and measure the fine structure of the P states, which can be characterized by the ratio of mass splittings within the triplet: $r \equiv (M_{J=2} - M_{J=1}) / (M_{J=1} - M_{J=0})$. Averaging the values of $r(2P)$ from several experiments [rather than determining $r(2P)$ from the world average of the photon energies], the ratio of mass splittings measured in $Y(3S)$ radiative transitions to the $\chi_{b,J}(2P)$ triplet is determined to be $r(2P) = 0.576 \pm 0.014$ [7]. Phenomenologically, the parameter r gives information on the Lorentz transformation properties of the $b\bar{b}$ confining potential; different predictions for r result from different assumptions about the relative vector and scalar contributions. The tabulated world average for the ratio of mass splittings measured

for the $\chi_{b,J}(1P)$ triplet is $r(1P) = 0.65 \pm 0.03$ [7], corresponding to $r(2P) < r(1P)$, opposite to most model predictions [7,8].

These data were obtained with the CLEO II detector [9] at the Cornell Electron Storage Ring (CESR) corresponding to an integrated luminosity of 73.6 pb^{-1} at the $Y(2S)$ energy. Based on the number of hadronic events measured at this energy, we determine that this luminosity is equivalent to a total number of $(488 \pm 18) \times 10^3$ produced $Y(2S)$ events. The advantage of the present analysis over previous analyses lies primarily in the high segmentation of the CLEO II calorimeter, which offers improved resolution of individual photon showers, with excellent solid angle coverage.

Candidate events are required to have at least three observed charged tracks in the event, with a total visible energy greater than the single electron (or positron) beam energy. Additional criteria are imposed to minimize contamination to our photon spectrum from non-hadronic events, such as beam-gas, beam-wall, or two-photon collisions [10]. We note that such backgrounds contribute only a smooth background to our observed photon energy spectrum.

Only photons from the barrel region ($|\cos \theta_\gamma| < 0.7$, with θ_γ the polar angle of the shower) are considered in this analysis. The fractional energy resolution for photons in the barrel region of the calorimeter [$(\sigma_E/E) \approx 5\%$ for $E_\gamma = 130 \text{ MeV}$] is approximately twice as good as in the end cap regions. Photon candidates are required to be well separated from charged tracks and other photon candidates in the same event. The lateral shower shape is required to be consistent with that expected from a true photon, and inconsistent with the energy deposition patterns expected for charged particles. Showers from “hot spots” in the calorimeter are flagged on a run-by-run basis and eliminated from consideration as inclusive photon candidates.

The photon energy scale is set by a three-stage calorimeter calibration procedure [9,10]. Pulsing of the readout electronics enables determination of the pedestals and gains characteristic of each channel, independent of the crystal light output. The energy calibrations for individual crystals are then calculated using reconstructed showers matched to beam-energy electrons in Bhabha events; the factors which convert normalized crystal light output to energy deposition, one per crystal, are obtained by minimizing the rms width of the electron shower energy distribution and constraining it to peak at the beam energy. The third and final stage of calibration guarantees that any monochromatic photon energy spectrum peaks at the incident photon energy, effectively correcting for any non-linearity in the crystal response,

*Permanent address: Lawrence Livermore National Laboratory, Livermore, CA 94551.

†Permanent address: BINP, RU-630090 Novosibirsk, Russia.

‡Permanent address: Yonsei University, Seoul 120-749, Korea.

§Permanent address: Brookhaven National Laboratory, Upton, NY 11973.

||Permanent address: University of Texas, Austin, TX 78712.

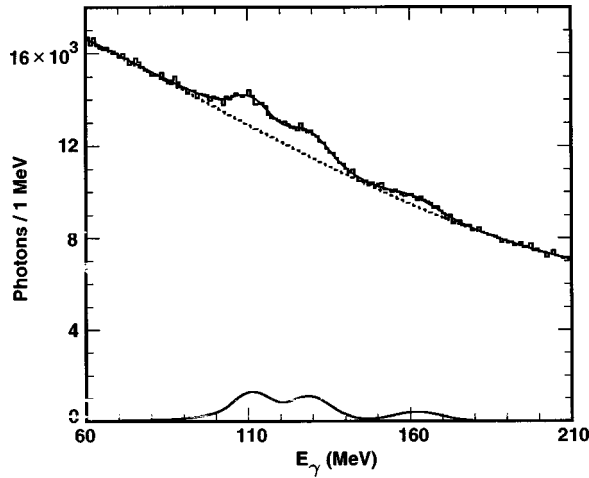


FIG. 1. Fit to the inclusive spectrum of photon candidates for the $Y(2S)$ data set. Also shown is the signal function used in the fit.

shower leakage from the cesium iodide, or bias in the reconstruction algorithm. This absolute energy calibration selects photon candidates that can be kinematically constrained, using radiative Bhabha ($ee\gamma$), $\gamma\gamma$ ($\gamma\gamma\gamma$), and muon pair ($\mu\mu\gamma$) events for photons above 0.5 GeV and π^0 's below 2.5 GeV. Most relevant to this analysis is the π^0 calibration, which requires consistency between the observed $\pi^0 \rightarrow \gamma\gamma$ mass peak and the expected mass. The π^0 calibration accounts for the contributions to the observed π^0 mass line shape from energy-dependent shower angle and energy resolutions of both its constituent photons. The correction amounts to $\sim 1\%$ near 100 MeV, and varies slowly and continuously with energy. The $ee\gamma$, $\mu\mu\gamma$, $\gamma\gamma\gamma$, and π^0 samples yield compatible corrections in the energy regions where they can be compared with one another. For the energy regime in this analysis we assess the uncertainty in the overall absolute energy scale to be $\pm 0.4\%$.

After applying all event selection requirements and photon criteria, we obtain the inclusive photon spectrum shown in Fig. 1, with a fit to signal plus background overlaid. Three enhancements are visible in this distribution above a smooth background. We attribute the lower energy photon peak to $Y(2S) \rightarrow \gamma\chi_{b,2}(1P)$, the middle peak to $Y(2S) \rightarrow \gamma\chi_{b,1}(1P)$, and the highest energy peak to the $Y(2S) \rightarrow \gamma\chi_{b,0}(1P)$ transition. The smooth background is primarily due to $\pi^0 \rightarrow \gamma\gamma$ photons, as well as non-photon showers which passed the photon selection criteria. We fit this background shape using a third order polynomial.

The signal shape is parametrized using a functional form originally used by the Crystal Ball Collaboration [11]. This is a nearly Gaussian distribution with a tail at lower energies to take into account longitudinal and transverse shower leakage in the calorimeter. The expected ratios of the linewidths (i.e., the shape of the resolution curve as a function of photon energy) are fixed from Monte Carlo simulations; to account for the possibility that the Monte Carlo simulation may not exactly reproduce the overall absolute resolution, the width of one of the lines (arbitrarily chosen to be the $J=1$ state) is allowed to float in the fit. Since the intrinsic widths of the $\chi_{b,J}(1P)$ states are expected to be of order ≤ 1 MeV, the

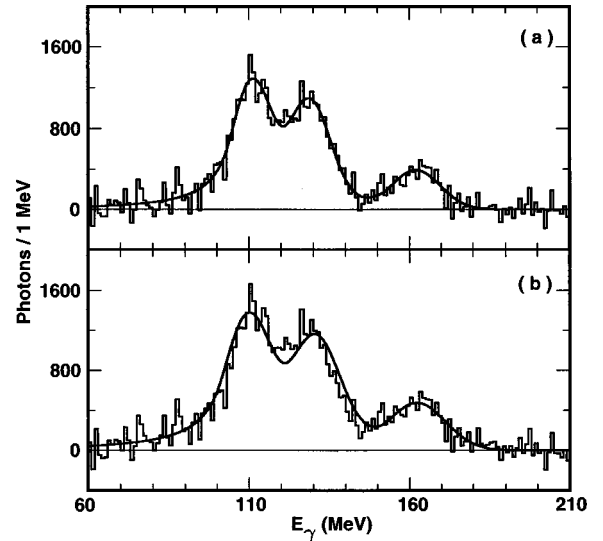


FIG. 2. Background subtracted photon energy spectrum, showing results of a free fit (top curve overlaying the histogram), and also overlay of the signal function curve obtained by constraining the masses of the $\chi_{b,J}(1P)$ states to their previously tabulated values (bottom).

experimental resolution should dominate the observed line-width. The aggregate signal function therefore has seven free parameters: the three line positions, their areas, and the energy resolution of the middle photon line. The spectrum of photon candidates after the third order polynomial is subtracted is shown in Fig. 2(a), with the aggregate signal function overlaid. The results of the fit are given in Table I (only statistical errors are presented). In Fig. 2(b), we have superimposed upon the background-subtracted spectrum the signals that would be expected, using the presently tabulated values for the masses of the $\chi_{b,J}(1P)$ states [12]. It is clear that this results in an inferior fit. Our background-subtracted data are obviously incompatible with the presently tabulated $\chi_{b,J}(1P)$ masses. To properly include correlations between the measured photon line energies in determination of $r(1P)$, we perform an additional fit using the same signal function but using a different set of free parameters: two line positions, $r(1P)$, the area of one line and two ratios of the matrix elements (before efficiency correction). From this fit, identical to the fit shown in Fig. 2(a), $r(1P)$ is determined to be 0.542 ± 0.022 . The statistical error in $r(1P)$ is obtained from this fit rather than by propagating errors from the measured $\chi_{b,J}(1P)$ line positions. In this way, systematic uncertainties cancel in our extraction of $r(1P)$.

TABLE I. Energies, raw yields (from fit to data photon spectrum) and efficiencies (from Monte Carlo simulations, and including J -dependent geometric acceptances) for $Y(2S) \rightarrow \gamma\chi_{b,J}(1P)$ transitions. Errors shown are statistical only.

| Transition | E_γ (MeV) | Yield (N_γ) | Efficiency (%) |
|------------|------------------|----------------------|----------------|
| $J=2$ | 110.8 ± 0.3 | 20723 ± 1436 | 57.1 ± 5.2 |
| $J=1$ | 128.8 ± 0.4 | 20806 ± 1466 | 61.8 ± 5.9 |
| $J=0$ | 162.0 ± 0.8 | 8637 ± 1274 | 52.4 ± 7.1 |

TABLE II. Evaluation of the total systematic errors.

| Uncertainty in: | Calibration error | Selection | Fitting | Energy resolution (efficiency) | Number of Y(2S) produced | Total |
|---|-------------------|-----------|---------|--------------------------------|--------------------------|-------|
| $J=2$ line position (MeV) | 0.40 | 0.27 | 0.31 | 0.22 | – | 0.6 |
| $J=1$ line position (MeV) | 0.42 | 0.26 | 0.29 | 0.10 | – | 0.6 |
| $J=0$ line position (MeV) | 0.45 | 0.62 | 0.79 | 0.49 | – | 1.2 |
| r | 0.001 | 0.012 | 0.009 | 0.019 | – | 0.024 |
| $\mathcal{B}(Y(2S) \rightarrow \gamma\chi_{b,2})$ (%) | – | 4.6 | 2.8 | 9.1 | 3.7 | 11.2 |
| $\mathcal{B}(Y(2S) \rightarrow \gamma\chi_{b,1})$ (%) | – | 5.9 | 4.7 | 9.5 | 3.7 | 12.7 |
| $\mathcal{B}(Y(2S) \rightarrow \gamma\chi_{b,0})$ (%) | – | 10.3 | 9.1 | 13.5 | 3.7 | 19.6 |
| $\frac{ \langle\chi_{b,2}(1P) R 2S\rangle ^2}{ \langle\chi_{b,1}(1P) R 2S\rangle ^2}$ | – | 0.055 | 0.096 | 0.010 | – | 0.11 |
| $\frac{ \langle\chi_{b,0}(1P) R 2S\rangle ^2}{ \langle\chi_{b,1}(1P) R 2S\rangle ^2}$ | – | 0.041 | 0.230 | 0.110 | – | 0.26 |

We use a GEANT-based, full CLEO II Monte Carlo simulation to determine the photon finding efficiency for each transition line, as presented in Table I. The geometric acceptance is calculated for each transition using the appropriate polar angular distributions for transitions to the $J=2$ ($dN/d \cos \theta_\gamma \propto 1 + \frac{1}{13} \cos^2 \theta_\gamma$), $J=1$ ($dN/d \cos \theta_\gamma \propto 1 - \frac{1}{3} \cos^2 \theta_\gamma$), and $J=0$ ($dN/d \cos \theta_\gamma \propto 1 + \cos^2 \theta_\gamma$) states, respectively. We use the overall efficiency (including both photon reconstruction and geometric acceptance) appropriate for each transition (Table I) to calculate the branching fractions from the $Y(2S)$ to the $\chi_{b,j}(1P)$ triplet states (Table III).

In addition to the systematic error due to the calorimeter calibration, primary systematic errors are due to event and photon selection and the signal extraction procedure, as summarized in Table II. The photon selection systematic is evaluated by remeasuring the photon spectrum using different definitions of ‘‘photons.’’ We estimate the signal extraction systematic by using a variety of signal parametrizations (using a bifurcated Gaussian rather than the Crystal Ball line shape, e.g.) and different parametrizations for the background under the signal. The uncertainty in the energy resolution is found to be the largest systematic error contributing to the total systematic error of $r(1P)$. The errors in the efficiencies are also dominated by the uncertainty in the energy resolution and are correspondingly propagated into systematic errors of the branching fractions (if the Monte Carlo simulation has better resolution than in data, e.g., then the Monte Carlo signals are too narrow and the corresponding efficiencies underestimated). The larger overall systematic

error for the $J=0$ line is attributable to the closer proximity of the minimum ionizing peak for this line compared to the two lower energy lines (and, hence, greater sensitivity to photon selection requirements designed to suppress showers from charged tracks) and a greater uncertainty in the extrapolated energy resolution at this energy.

As a cross-check on the extracted value of r , we have conducted a parallel analysis, in which we search for photons in the ‘‘exclusive’’ mode. In this case, we fully reconstruct the decay chain: $Y(2S) \rightarrow \chi_{b,j}(1P) \gamma$, $\chi_{b,j}(1P) \rightarrow \gamma Y(1S)$, $Y(1S) \rightarrow l^+ l^-$, for which $l^+ l^-$ is $e^+ e^-$ or $\mu^+ \mu^-$. This very distinctive final state topology consists of two leptons and two photons. Unfortunately, because of the very small branching fraction for $\chi_{b,0}(1P) \rightarrow \gamma Y(1S)$, these exclusive events cannot be used to completely determine $r(1P)$. Nevertheless, we find that the measured mass difference between the $J=2$ and $J=1$ states from our exclusive data ($\Delta M = 129.9 \pm 0.7 - 111.0 \pm 1.1$ MeV = 18.9 ± 1.3 MeV, statistical errors only) is in agreement with the mass difference measured in the inclusive mode ($\Delta M = 18.0 \pm 1.0$ MeV, as computed from Table III). We can also combine the masses observed for the $J=2$ and $J=1$ states in the exclusive mode with the mass measured for the $J=0$ state in the inclusive mode to obtain a value of r' ; the prime here indicates that this quantity is derived from a combination of the exclusive and the inclusive measurements. We obtain $r' = 0.59 \pm 0.05$ (statistical errors only), consistent with the value we obtained from the inclusive data. We do not include these exclusive results in our final determination of $r(1P)$ owing to their relatively small statistical weight compared to the inclusive sample.

TABLE III. $Y(2S) \rightarrow \gamma X$ transition energies and branching fractions (\mathcal{B}).

| Transition | E_γ (this expt.) (MeV) | E_γ PDG [12] (MeV) | $M(\chi_{b,j})(1P)$ (this expt.) (MeV) | \mathcal{B} (this expt.) (%) | PDG [12] (%) |
|------------|-------------------------------|---------------------------|--|--------------------------------|---------------|
| $J=2$ | $110.8 \pm 0.3 \pm 0.6$ | 109.6 ± 0.6 | $9911.9 \pm 0.3 \pm 0.6$ | $7.4 \pm 0.5 \pm 0.8$ | 6.6 ± 0.9 |
| $J=1$ | $128.8 \pm 0.4 \pm 0.6$ | 130.6 ± 0.7 | $9893.7 \pm 0.4 \pm 0.6$ | $6.9 \pm 0.5 \pm 0.9$ | 6.7 ± 0.9 |
| $J=0$ | $162.0 \pm 0.8 \pm 1.2$ | 162.3 ± 1.3 | $9860.0 \pm 0.8 \pm 1.2$ | $3.4 \pm 0.5 \pm 0.6$ | 4.3 ± 1.0 |

TABLE IV. Ratios of $\Gamma_{E1}/[E_\gamma^3(2J+1)]$.

| | $\frac{ \langle\chi_{b,2}(1P) R 2S\rangle ^2}{ \langle\chi_{b,1}(1P) R 2S\rangle ^2}$ | $\frac{ \langle\chi_{b,0}(1P) R 2S\rangle ^2}{ \langle\chi_{b,1}(1P) R 2S\rangle ^2}$ |
|----------------------------|---|---|
| This experiment | $1.02 \pm 0.06 \pm 0.11$ | $0.75 \pm 0.09 \pm 0.26$ |
| Previous world average [7] | 0.92 ± 0.11 | 0.95 ± 0.16 |

We summarize the results for the photon energies from our inclusive analysis and compare our results with the present Particle Data Group averages in Table III. Based on the PDG value for $M_{Y2S} = 10023.3$ MeV, we have also tabulated the $\chi_{b,J}(1P)$ masses inferred from our measured photon energies. We similarly compare our results for the branching fractions with previous measurements in Table III. We find $r(1P)$ to be $0.542 \pm 0.022 \pm 0.024$, inconsistent with the previous world average of 0.65 ± 0.03 . Note that r is insensitive to an overall miscalibration of the photon energy scale.

The widths for the electric dipole transitions $Y(2S) \rightarrow \gamma\chi_{b,J}(1P)$ are given in terms of the characteristic interquark separation R by

$$\Gamma_{E1} = \mathcal{B}\Gamma_{tot} = \frac{4}{27} \alpha e_b^2 E_\gamma^3 (2J+1) |\langle 1P|R|2S\rangle|^2.$$

In this equation, α is the electromagnetic coupling constant, e_b is the charge of the b quark, and $\langle 1P|R|2S\rangle$ is the matrix element. By averaging over the transitions to all three $\chi_{b,J}(1P)$ states and using $\Gamma_{tot}(2S) = (44.0 \pm 7.0)$ keV [12], we find $\langle 1P|R|2S\rangle = (1.91 \pm 0.22)$ GeV⁻¹, in which the error includes both statistical and systematic errors. This can be compared to the world average $\langle 1P|R|2S\rangle = (1.9 \pm 0.2)$ GeV⁻¹ [7].

By determining the ratios of the transition widths for states having different total angular momentum J , we can cancel the uncertainty due to the total $Y(2S)$ width. Ratios

of the squared matrix element for different J values are equal to ratios of the quantity $\Gamma_{E1}/[E_\gamma^3(2J+1)]$. To include correlations between photon line amplitudes, the fit to the photon energy spectrum was repeated with ratios of the amplitudes as free parameters. We present our experimental results and the previous world average for ratios of $\Gamma_{E1}/[E_\gamma^3(2J+1)]$ in Table IV. Theoretically these ratios are expected to be 1.0 in the non-relativistic limit. Spin dependence of the matrix element is introduced by relativistic corrections. Although calculations vary, all models predict that the J -dependent corrections follow: $|\langle\chi_{b,2}(1P)|R|2S\rangle|^2 > |\langle\chi_{b,1}(1P)|R|2S\rangle|^2 > |\langle\chi_{b,0}(1P)|R|2S\rangle|^2$ [7].

Based on the inclusive measurement of photon energies taken from $Y(2S)$ data, we have measured the branching fractions from the $Y(2S)$ state to the $\chi_{b,J}$ triplet, as well as the masses of the states in the triplet. We find the ratio of mass splittings, $r(1P) \equiv (M_{J=2} - M_{J=1}) / (M_{J=1} - M_{J=0}) = 0.542 \pm 0.022 \pm 0.024$, substantially lower than the previous world average, but consistent with the expectation that $r(1P) < r(2P)$.

We gratefully acknowledge the effort of the CESR staff in providing us with excellent luminosity and running conditions. This work was supported by the National Science Foundation, the U.S. Department of Energy, Research Corporation, the Natural Sciences and Engineering Research Council of Canada, the A. P. Sloan Foundation, the Swiss National Science Foundation, and the Alexander von Humboldt Stiftung.

- | | |
|--|--|
| <p>[1] CUSB Collaboration, C. Klopfenstein <i>et al.</i>, Phys. Rev. Lett. 51, 160 (1983).</p> <p>[2] CLEO Collaboration, P. Haas <i>et al.</i>, Phys. Rev. Lett. 52, 799 (1984).</p> <p>[3] Crystal Ball Collaboration, R. Nernst <i>et al.</i>, Phys. Rev. Lett. 54, 2195 (1985).</p> <p>[4] ARGUS Collaboration, H. Albrecht <i>et al.</i>, Phys. Lett. 160B, 331 (1985).</p> <p>[5] CUSB Collaboration, F. Pauss <i>et al.</i>, Phys. Lett. 130B, 439 (1983).</p> <p>[6] Crystal Ball Collaboration, W. Walk <i>et al.</i>, Phys. Rev. D 34, 2611 (1986).</p> <p>[7] D. Besson and T. Skwarnicki, Annu. Rev. Nucl. Part. Sci. 43, 333 (1993), and references cited therein.</p> | <p>[8] S. Gupta, S. Radford, and W. Repko, Phys. Rev. D 34, 201 (1986); H. Ito, Prog. Theor. Phys. 84, 94 (1990); R. McClary and N. Byers, Phys. Rev. D 28, 1692 (1983); J. Carlson, J. Kogut, and V. Pandharipande, <i>ibid.</i> 28, 2807 (1983); W. Büchmüller, Phys. Lett. 79B, 112 (1982).</p> <p>[9] CLEO II, Y. Kubota <i>et al.</i>, Nucl. Instrum. Methods Phys. Res. A 320, 66 (1992).</p> <p>[10] CLEO II Collaboration, R. Morrison <i>et al.</i>, Phys. Rev. Lett. 67, 1696 (1991).</p> <p>[11] Tomasz Skwarnicki, Ph.D. thesis, Institute of Nuclear Physics, Krakow, 1986, DESY internal report DESY F31-86-02 (unpublished).</p> <p>[12] Particle Data Group, R. M. Barnett <i>et al.</i>, Phys. Rev. D 54, 1 (1996).</p> |
|--|--|